

# Sensor Fusion - Final Project

Adrian Pfisterer

## I. INTRODUCTION

In recent years Inertial Measurement Units (IMUs) have become widely popular for tracking the motion of kinematic chains. This is mainly due to their low cost and small form factor as well as advances in sensor fusion algorithms. While attached to rigid segments of a kinematic chain, IMUs provide inertial 9D measurements consisting of 3D accelerometer, 3D magnetometer, and 3D gyroscope data. Especially magnetometer readings are prone to inaccuracies when used in indoor environments or close to other electronic devices. When omitting the magnetometer and relying solely on accelerometer and gyroscope readings, valuable heading information is lost. To overcome this issue often kinematic constraints are introduced to correct the heading. This approach is also applicable when using distorted magnetometer data. Kinematic constraints can also be used to overcome issues such as bias drift.

The aim of this abstract is to compare two 9D IMU sensor fusion approaches with a 6D magnetometer free method. In addition, the potential of exploiting kinematic constraints to improve position estimates is explored. Results are presented based on measurements of two IMUs mounted on a robotic arm (Fig. 1) performing a drawing motion in the  $x$ - $y$  plane.

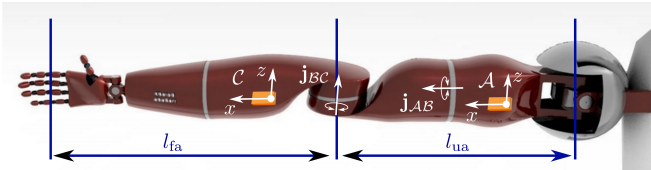


Fig. 1. An illustration of the robotic arm showing IMUs  $\mathcal{A}$  and  $\mathcal{C}$  which are mounted s.t. their local  $x$ -axis coincides with the longitudinal axis of their respective segment. Both segments are connected by two revolute joints  $\mathbf{j}_{BC}$  and  $\mathbf{j}_{AB}$  allowing for flexion/extension (FE) and pronation/supination (PS) respectively.

## II. METHOD

### A. Sensor Fusion

A 9D sensor fusion algorithm proposed by Seel and Ruppig [4] is used to estimate the orientation of both IMUs. Consider the orientation of IMU  $\mathcal{A}$  with respect to an inertial reference frame  $\mathcal{E}$  with vertical axis  $\mathcal{E}\mathbf{r}_{acc}$  and horizontally northbound axis  $\mathcal{E}\mathbf{r}_{mag}$ . The corresponding accelerometer and magnetometer readings within the local  $\mathcal{A}$  frame are denoted with  $\mathcal{A}\mathbf{a}(t)$  and  $\mathcal{A}\mathbf{m}(t)$  respectively. The disagreement between accelerometer/magnetometer measurements and an arbitrary orientation  $\mathcal{E}^{\mathcal{A}}\mathbf{q}$  can then be expressed by transforming

both reference vectors  $\mathcal{E}\mathbf{r}_{acc}$  and  $\mathcal{E}\mathbf{r}_{mag}$  into the  $\mathcal{A}$  frame:

$$f_{acc}(\mathcal{E}^{\mathcal{A}}\mathbf{q}) = \|(\mathcal{E}^{\mathcal{A}}\mathbf{q})^* \otimes \mathcal{E}\mathbf{r}_{acc} \otimes \mathcal{E}^{\mathcal{A}}\mathbf{q} - \mathcal{A}\mathbf{a}(t)\|_2, \quad (1)$$

$$f_{mag}(\mathcal{E}^{\mathcal{A}}\mathbf{q}) = \|(\mathcal{E}^{\mathcal{A}}\mathbf{q})^* \otimes \mathcal{E}\mathbf{r}_{mag} \otimes \mathcal{E}^{\mathcal{A}}\mathbf{q} - \mathcal{A}\mathbf{m}(t)\|_2. \quad (2)$$

Here  $\otimes$  denotes the quaternion product and  $*$  the inverse quaternion. The gyroscope prediction is then rotated by a small weighted portion into the direction of the orientations  $\mathbf{q}_{corr,acc}$  and  $\mathbf{q}_{corr,mag}$  that minimize (1) and (2). The correction using  $\mathbf{q}_{corr,mag}$  is projected into the horizontal plane to ensure that only the heading component is affected. Prediction and correction steps are then applied for each sampling interval. 9D Sensor fusion can also be achieved by using an Extended Kalman Filter (EKF) [5] along with the following nonlinear state and measurement models for each time instance  $k$ :

$$\mathbf{x}_k = f(\mathbf{x}_{k-1}, \mathbf{g}_k) = \begin{bmatrix} \mathbf{q}_k + \mathbf{v}_k \\ \mathbf{b}_{k-1} \end{bmatrix}, \quad (3)$$

$$\mathbf{q}_k = \mathbf{q}_{k-1} \otimes \begin{bmatrix} \cos(\frac{1}{2}\|\mathbf{g}_k + \mathbf{b}_{k-1}\|_2 T_s) \\ \sin(\frac{1}{2}\|\mathbf{g}_k + \mathbf{b}_{k-1}\|_2 T_s) \frac{\mathbf{g}_k + \mathbf{b}_{k-1}}{\|\mathbf{g}_k + \mathbf{b}_{k-1}\|_2} \end{bmatrix}, \quad (4)$$

$$\mathbf{y}_k = h(\mathbf{x}_k) = \begin{bmatrix} (\mathbf{q}_k)^* \otimes \mathcal{E}\mathbf{r}_{acc} \otimes \mathbf{q}_k \\ (\mathbf{q}_k)^* \otimes \mathcal{E}\mathbf{r}_{mag} \otimes \mathbf{q}_k \end{bmatrix} + \mathbf{w}_k. \quad (5)$$

The gyroscope reading at sampling interval  $k$  is expressed by  $\mathbf{g}_k$  while  $\mathbf{v}_k$  and  $\mathbf{w}_k$  are zero-mean Gaussian white noise sequences and  $T_s$  is the sample time. Using (3) and (5) the EKF estimates the orientation  $\mathbf{q}_k$  as well as the gyroscope bias  $\mathbf{b}_k$ .

Both 9D Sensor fusion approaches proposed here can be modified to provide 6D orientation estimates by omitting magnetometer measurements in (2) and (5).

### B. Kinematic Constraints

Often the sensor fusion methods stated above yield results that are still subject to inaccuracies and disturbances. Especially when magnetometer free 6D sensor fusion is utilized, the lack of heading information needs to be compensated. This can be expressed analogously to Laidig et al. [1] by introducing new reference frames for a two segment kinematic chain  $\mathcal{E}_1$  and  $\mathcal{E}_2$  in addition to  $\mathcal{E}$ . Here  $\mathcal{E}_1$  and  $\mathcal{E}_2$  are rotated by an heading error  $\delta(t)$  around the global  $z$ -axis. Their relative orientation is then defined as:

$$\mathcal{E}_2^{\mathcal{E}_1}\mathbf{q} = \begin{bmatrix} \cos(\frac{\delta}{2}) & 0 & 0 & \sin(\frac{\delta}{2}) \end{bmatrix}^T. \quad (6)$$

Another constraint introduced by Laidig et al. [1] can be used to determine the joint axes of a kinematic chain consisting of two segments and two joints with axes  $\mathbf{j}_{AB}$  and  $\mathbf{j}_{BC}$  such as the robotic arm in Fig. 1. The gyroscope measurements  $\mathcal{A}\mathbf{g}(t)$  and  $\mathcal{C}\mathbf{g}(t)$  of each inertial sensor  $\mathcal{A}$  and  $\mathcal{C}$  must fulfill the

following scalar product when transformed into the global frame  $\mathcal{E}$ :

$$e_k = (\mathcal{C}\mathbf{g}(t) - \mathcal{A}\mathbf{g}(t)) \cdot (\varepsilon\mathbf{j}_{BC} - \varepsilon\mathbf{j}_{AB}) = 0. \quad (7)$$

This needs to hold for every time instant  $k \in [1, N]$  if  $\delta(t) = 0$  and can therefore be formulated as sum of squares (SSQ) minimization problem  $\mathbf{e}^T\mathbf{e}$  with error vector  $\mathbf{e} = [e_1 \ e_2 \ \dots \ e_N]^T$ . Minimizing the SSQ using e.g., the Levenberg-Marquardt algorithm [2] yields an estimate for the unit length vectors  $\mathbf{j}_{AB}$  and  $\mathbf{j}_{BC}$ .

When virtually replacing the revolute joint  $\mathbf{j}_{BC}$  with a spherical one  $\mathbf{o}$  and therefore omitting joint  $\mathbf{j}_{AB}$ , a constraint proposed by Seel et al. [3] can be exploited to estimate the position of the joint center  $\mathbf{o}_A$  and  $\mathbf{o}_C$  in each sensor frame respectively. Denote the accelerations of each IMU  $\mathcal{A}\mathbf{a}(t)$  and  $\mathcal{C}\mathbf{a}(t)$  while the corresponding gyroscope readings are  $\mathcal{A}\mathbf{g}(t)$  and  $\mathcal{C}\mathbf{g}(t)$ . Then

$$\begin{aligned} e(t) &:= \|\mathcal{A}\mathbf{a}(t) - \mathbf{\Gamma}_{\mathcal{A}\mathcal{g}}(\mathbf{o}_A)\|_2 \\ &\quad - \|\mathcal{C}\mathbf{a}(t) - \mathbf{\Gamma}_{\mathcal{C}\mathcal{g}}(\mathbf{o}_C)\|_2 = 0, \\ \mathbf{\Gamma}_{ig}(\mathbf{o}_i) &:= i\mathbf{g}(t) \times (i\mathbf{g}(t) \times \mathbf{o}_i) + i\dot{\mathbf{g}}(t) \times \mathbf{o}_i, \\ i &= \mathcal{A}, \mathcal{C}. \end{aligned} \quad (8)$$

As before minimizing the SSQ  $\mathbf{r}^T\mathbf{r}$  with  $\mathbf{r} = [e(t_1) \ e(t_2) \ \dots \ e(t_n)]^T$  provides estimates for  $\mathbf{o}_A$  and  $\mathbf{o}_C$ .

### III. RESULTS

The 9D sensor fusion algorithm proposed by Seel and Ruppig [4] is compared with a 9D EKF approach. The former method does not compensate for gyroscope bias, therefore the bias is estimated during a resting pose. For both approaches, it is assumed that the magnetometer measurements are undistorted. In addition, 6D EKF sensor fusion is compared against both 9D methods. Since no magnetometer information is available for 6D sensor fusion, the heading offset  $\delta$  is determined using a known elbow i.e., FE joint angle at the end of the motion. Afterwards the relative heading angle is assumed to be constant and is corrected using (6).

In Fig. 2 the wrist position estimates for all approaches are shown. All wrist trajectories are computed by exploiting the constraint that both arm segments are rigidly connected to each other and have specific lengths  $l_{fa}$  and  $l_{ua}$ . In addition,

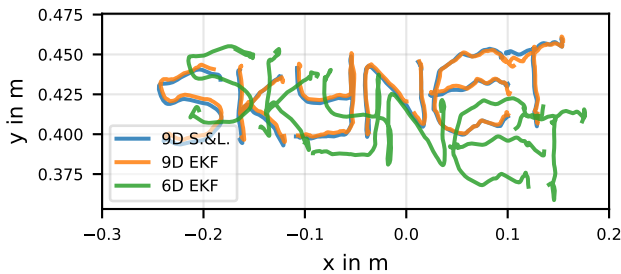


Fig. 2. Robot's wrist trajectory projected into the  $x$ - $y$  plane with a threshold of  $z \in [0.008\text{m}, 0.022\text{m}]$

the elbow joint's carrying angle estimates during the motion

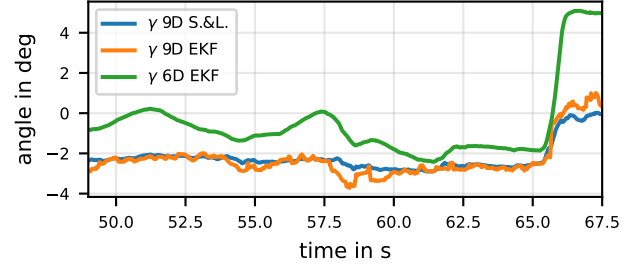


Fig. 3. Elbow joint  $\mathbf{j}_{BC}$  carrying angle  $\gamma$  over time computed by decomposing the relative quaternion  ${}^{\mathcal{A}}\mathbf{q}$  between the  $\mathcal{A}$  and  $\mathcal{C}$  frame using  $x$ - $z'$ - $y''$  Euler angle convention i.e.  $\alpha$ - $\gamma$ - $\beta$

are illustrated in Fig. 3. The joint axis  $\mathcal{C}\mathbf{j}_{BC}$  in  $\mathcal{C}$  frame coordinates is computed by minimizing the SSQ problem (7) and using the assumption that  $\mathcal{A}\mathbf{j}_{AB} = [1 \ 0 \ 0]^T$ . Analogously, vectors  $\mathbf{o}_A$  and  $\mathbf{o}_C$  are calculated using (8). They are used to determine the distance between the elbow joint center and the origins of frame  $\mathcal{A}$  and  $\mathcal{C}$  respectively. Both distances are stated in Table I along with the joint axis  $\mathcal{C}\mathbf{j}_{BC}$  estimate.

	$j_{BC,x}$	$j_{BC,y}$	$j_{BC,z}$	$\ \mathbf{o}_A\ _2$	$\ \mathbf{o}_C\ _2$
9D Seel & Ruppig	-0.003m	0.999m	0.045m	0.102m	0.17m
9D EKF	0.028m	0.991m	0.133m	0.102m	0.17m
6D EKF	0.14m	0.934m	0.315m	0.102m	0.17m

TABLE I

### IV. CONCLUSION

It could be shown that all approaches proposed yield acceptable results and enable sufficient reconstruction of the drawing motion. Furthermore, the 9D sensor fusion approach by Seel and Ruppig is superior to both EKF methods. This is particularly evident in the carrying angle estimation. However, it should be noted that Seel and Ruppig's method requires prior gyroscope bias removal in contrast to the 9D EKF. The results using the 6D EKF with heading correction demonstrate that position estimation without magnetometer information is possible but not as accurate as full 9D sensor fusion. Here estimates can be improved further by introducing additional kinematic constraints and estimate the heading error  $\delta$  as a function of time. Clearly, it was demonstrated how important it is to take full advantage of all information available.

### REFERENCES

- [1] Daniel Laidig, Philipp Müller, and Thomas Seel. Automatic anatomical calibration for IMU-based elbow angle measurement in disturbed magnetic fields. *Current Directions in Biomedical Engineering*, 3(2):167–170, 2017.
- [2] Jorge J Moré. The Levenberg-Marquardt algorithm: implementation and theory. In *Numerical analysis*, pages 105–116. Springer, 1978.
- [3] T. Seel, T. Schauer, and J. Raisch. Joint axis and position estimation from inertial measurement data by exploiting kinematic constraints. In *2012 IEEE International Conference on Control Applications*, pages 45–49, 2012.
- [4] Thomas Seel and Stefan Ruppig. Eliminating the effect of magnetic disturbances on the inclination estimates of inertial sensors. *IFAC-PapersOnLine*, 50(1):8798–8803, 2017. 20th IFAC World Congress.
- [5] S. Thrun, W. Burgard, D. Fox, and R.C. Arkin. *Probabilistic Robotics*. Intelligent Robotics and Autonomous Agents series. MIT Press, 2005.